

## Structure and Stratigraphy Beneath a Young Phreatic Vent: South Inyo Crater, Long Valley Caldera, California

JOHN C. EICHELBERGER,<sup>1</sup> THOMAS A. VOGEL,<sup>2</sup> LELAND W. YOUNKER,<sup>3</sup> C. DAN MILLER,<sup>4</sup>  
GRANT H. HEIKEN,<sup>5</sup> AND KENNETH H. WOHLTZ<sup>5</sup>

An 861-m-long hole has been cored on a slanted trajectory that passed directly beneath South Inyo Crater in the west moat of Long Valley Caldera, California. The purpose of the hole was to investigate the magmatic behavior that led to surface deformation and phreatic activity during the 600-year-old eruption of the Inyo vent chain. The hole was sited 216 m southwest of the crater, passed beneath its center at a depth of 566 m, and terminated 79 m northeast of the crater center at a depth of 810 m. Metamorphic basement was encountered at a depth of 779 m. The volcanic and sedimentary sequence consists solely of post-Bishop Tuff caldera fill, including 319 m of moat basalt and 342 m of early rhyolite, and is nearly 900 m thinner than in a Unocal Corporation well 900 m to the southeast. Apparently, a major fault lies between the two holes and forms part of the western structural boundary of the caldera, 3–4 km inboard of its topographic boundary. Breccia zones that intrude the caldera fill were intersected at 12.0–9.3 m and 1.2–0.8 m SW and 8.5–25.1 m NE of the crater center. The largest breccia unit is symmetrically zoned from margins rich in vesicular rhyolite and locally derived rhyolite wall rock, with most clasts  $\leq 0.1$  m, to a center of up to 50 vol % basalt, with individual basalt clasts to 1 m in intersected length. The basalt appears to be an early feeder for the moat basalt sequence. The vesicular rhyolite is chemically distinct from both the rhyolite wall rock and previously recognized 600-year-old Inyo eruptives but matches fresh-appearing pyroclasts in the crater ejecta. This component of the breccia is therefore interpreted as representing juvenile magma that vesiculated and fragmented as it rose along the margins of an older basalt intrusion. During this process, wall rock fragments were ejected from depths extending to at least 800 m. Progression to a magmatic eruption was probably prevented by rapid influx of groundwater into the feeder. The chemical data do not support the hypothesis that a single, simple dike exists under the entire segment of the Inyo chain that was active 600 years ago. If such a dike exists, it apparently tapped different magma chambers along its ~10-km length. The excess of surface extension over that needed to accommodate the intruded juvenile material may reflect the presence of a larger intrusion at depth, below the level of fragmentation, or the contribution of tectonic activity to the surface deformation.

### INTRODUCTION

The Inyo Domes volcanic chain (Figure 1) is a 12-km line of mid- to late Holocene lava domes and phreatic craters that cuts northward across the northwest topographic margin of Long Valley Caldera [Miller, 1985; Bailey et al., 1976]. The trend of the chain is aligned approximately with the Hartley Springs fault, which has been active both before and after caldera collapse. During the most recent eruption about 600 years ago, three major magmatic vents, about a dozen phreatic vents, and numerous small faults were contemporaneously active along a line about 10 km long [Miller, 1985]. There was, however, a marked contrast in eruptive behavior between the northern and southern portions of the chain. Outside the caldera in the northern portion of the active segment, eruptions produced rhyolite to rhyodacite tephra deposits and lava domes and small phreatic craters [Miller, 1985; Fink, 1985]. Inside the caldera in the southern portion, three large phreatic craters formed and dramatic faulting and fracturing of the surface occurred [Mastin and Pollard, this issue]. Recognition that the linear array of vents was contemporaneously active

led to the hypothesis that the vents were fed from a common silicic dike [Miller, 1985; Fink and Pollard, 1983a, b]. It was further postulated that contrasting geologic conditions led to the contrast in eruptive behavior between the northern and southern segments [Eichelberger et al., 1985].

A program of research drilling (Figure 1) was undertaken to sample the intrusions beneath the Inyo chain and thereby test these hypotheses and investigate other aspects of magmatic behavior during intrusion and eruption [Eichelberger et al., 1984]. The work was funded by the Office of Basic Energy Sciences, U.S. Department of Energy, as part of the Continental Scientific Drilling Program. Drilling in the northern part of the chain confirmed the existence of a silicic dike at shallow depth between magmatic vents [Eichelberger et al., 1985]. Drilling of Inyo-4 beneath a phreatic crater in the southern part of the chain, the fourth and final hole of the series, provided a view of a very different magmatic environment. The basic observations and preliminary conclusions from Inyo-4 are the topic of this paper.

### STATE OF KNOWLEDGE PRIOR TO DRILLING INYO-4

The first phase of drilling showed the source dike for the Inyo eruption to be 6 m thick at a depth of 600 m midway between the Glass Creek and Obsidian Dome vents. The structure was found to broaden and become more complex under Obsidian Dome. At 400–500 m depth the conduit that fed the dome is 30 m thick and lies within a 50-m-wide zone of subsidiary intrusions and pyroclastic debris. Data on distribution of vesicles and retained volatiles in the system indicated that the magma had risen as an initially volatile-rich foam

<sup>1</sup>Sandia National Laboratories, Albuquerque, New Mexico.

<sup>2</sup>Department of Geological Sciences, Michigan State University, East Lansing.

<sup>3</sup>Lawrence Livermore National Laboratory, Livermore, California.

<sup>4</sup>Cascades Volcano Observatory, U.S. Geological Survey, Vancouver, Washington.

<sup>5</sup>Los Alamos National Laboratory, Los Alamos, New Mexico.

Copyright 1988 by the American Geophysical Union.

Paper number 8B2103.

0148-0227/88/008B-2103\$05.00

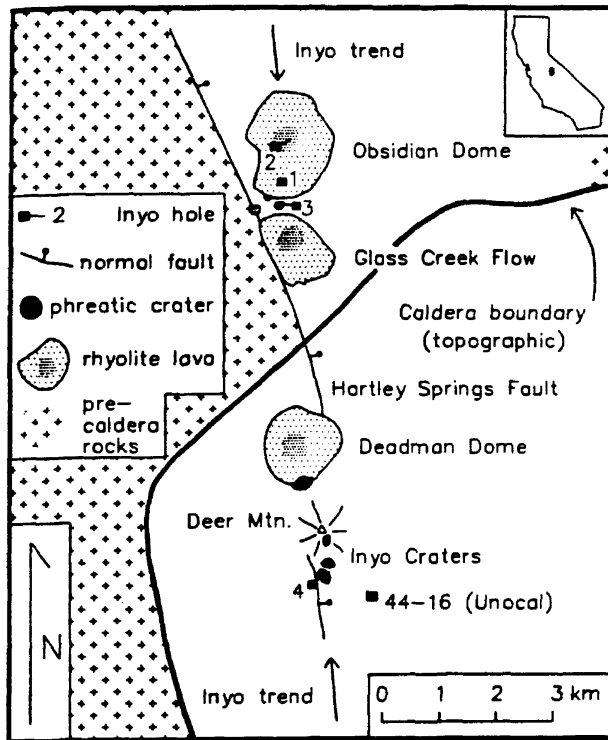


Fig. 1. Map showing major geologic features of the portion of the Inyo Domes chain that was active 600 years ago and environs. The densely shaded portions of the lava domes represent their elevated vent regions. The area of Long Valley Caldera shown is a part of the west moat, a low region between the west rim and resurgent dome. Locations of the Inyo research core holes (numbered) and the Unocal Corporation geothermal exploration hole are also shown. Precaldera rocks are Sierran granitic intrusives and metamorphic roof pendants, with subordinate areas of Tertiary lavas. Note that the Hartley Springs fault trends into the vicinity of Inyo-4 and Unocal 44-16.

[Eichelberger et al., 1986; Westrich et al., 1988]. The foam degassed by porous obsidian during extrusion. An important implication is that permeability of shallow wall rock controls degassing and hence eruptive behavior of magma.

It remained to discover whether the same dike is present at shallow depth beneath the southern portion of the chain, and if it is, why it did not reach the surface there but instead caused development of craters and fractures. The more permeable environment of the caldera could have promoted both more rapid cooling (by groundwater circulation) and more rapid degassing of the intruding magma. Both mechanisms would tend to stop the intrusion at depth, and both could lead to excavation of large craters over it. Such differences in cooling and degassing behavior of the dike system between the intracaldera and extracaldera environments could be assessed by comparing crystallinity and retained volatiles in core samples of the intrusion from the two settings. Alternatively, the controlling factor could have been mechanical. For example, the weaker rocks of the caldera may have inhibited upward migration of the dike [Reches and Fink, 1988]. The relationship of the dike to deformation of the wall rock and the surface could also be assessed by drilling. It was expected that the dike would be much thicker within the caldera because of the well-expressed surface deformation there.

#### DRILLING OF INYO-4

The objective for core hole Inyo-4 was therefore to intersect the intrusive feeder of the 600-year-old eruption at a location where the event produced phreatic activity and surface deformation rather than venting of magma. The hole was sited in the Inyo Craters area [Mastin and Pollard, this issue] where the Inyo trend lies farthest within Long Valley Caldera. The three large phreatic craters, the southernmost of which is South Inyo Crater, lie on a north-south line whose extension passes just east of the next Inyo vent to the north, Deadman Dome. Ejecta from the craters consists of blocks of mostly shallow derivation set in an extremely fine-grained matrix. The presence of uncharred wood and the muddy, indurated character of the matrix suggest wet, low-temperature conditions of emplacement. The deposits are typically a few meters thick at the crater rims, with blocks to 1 m in diameter, and thin rapidly away from their sources. Extending south from the craters is a zone of chaotically fractured ground. On either side and generally trending north-south are normal faults with vertical displacements up to 15 m. Those to the west of the crater trend are down to the east, whereas some of those to the east are down to the west, forming an asymmetrical graben. Measured (minimum) total extension across this zone of deformation is 10 m, and the estimated total extension is 40 m. The pattern and magnitude of displacements are consistent with analytical and scale models for surface deformation above a dike tens of meters thick whose top is a few hundred meters below the surface [Mastin and Pollard, this issue], or several times the thickness of the dike intersected by Inyo-3. A subsidiary trend splays off to the northwest from South Inyo Crater. It also consists of a central chaotically fractured graben and numerous, though smaller, phreatic craters.

South Inyo Crater is about 200 m in diameter and 60 m deep. It was chosen as the drilling target because it is the largest and most accessible crater and because its position at the intersection of two surface trends, both suggestive of shallow dikes, seemed to offer the highest probability of successfully intersecting an intrusive body. A site was chosen so that the azimuth of the hole, defined by the wellhead and the center of the crater lake, could be as close to perpendicular as possible to the main north-south trend of surface vents and faults. The chosen azimuth of N59°E makes an angle of 59° with the Inyo Craters trend and 73° with the subsidiary trend (Figure 2). The crater itself is actually elongate along the subsidiary trend rather than the main trend.

An initial dip for the hole was chosen so that the hole would intersect the target at approximately the same depth, 600 m, at which previous drilling had intersected the source dike beneath the northern portion of the chain. This choice was made to eliminate depth, and hence pressure, as a variable in comparing intrusive behavior between the two sites. For a straight hole, this would require a dip of 71°, but a dip of 67° was selected to compensate for the expected drooping trajectory. The actual path of the hole beneath the crater, as determined by a gyroscopic survey run after drilling, is shown in Figure 2. The droop was 1°/100 m, with no significant drift from the original azimuth. The hole passed under the center of the crater lake and intersected its target at the desired depth.

#### PRE-INYO STRATIGRAPHY

The Long Valley volcanic center [Bailey et al., 1976; Bailey, 1984] sits astride the structural boundary between the rela-

tively intact Sierra block and the extensional regime of the Basin and Range. Volcanism precursor to the caldera began about 3 Ma with eruption of mafic to intermediate-composition lavas and minor tephra from scattered vents. This activity generated a significant volcanic pile in what is now the western area of the caldera where Inyo-4 was sited. Silicic activity became significant at 2 Ma with eruption of the Glass Mountain complex (northeastern area of the present caldera) and climaxed at 0.7 Ma with eruption of 600 km<sup>3</sup> of rhyolite magma to form the Bishop Tuff. Contemporaneous subsidence of the source region for the tuff by as much as 3 km formed Long Valley Caldera. Collapse was quickly followed by resurgence of the west central caldera floor and by spatially and temporally coincident eruption of the aphyric early rhyolite flows and tuffs. This activity was complete by about 0.6 Ma. Markedly more porphyritic moat rhyolite began erupting in the caldera moat at 0.5 Ma and continued to 0.1 Ma with extrusion of Deer Mountain dome 1 km north of the Inyo-4 drill site. Overlapping this activity in time and space, moat "basalt" (includes more silicic associates) flows flooded the west moat of the caldera (0.2–0.1 Ma), and the Mammoth Mountain andesite to dacite volcano grew on the caldera's southwest margin. Holocene time marked the onset of Inyo chain activity [Wood, 1977]. The Inyo-4 lithologic log, which records a portion of this history, is shown in Figure 3.

**Moat basalt.** Twenty six lava flows and eight pyroclastic units were encountered by Inyo-4 within the moat basalt sequence. Additional units may be present in the first 18 m of the section that was not cored. Individual flows range in thickness from 1 to 31 m. All have vesicular tops, and some are vesicular throughout. Individual pyroclastic units range in thickness from 1 to 20 m. The lithologies are aphyric to microphyritic basalt to andesite and are increasingly silicic with decreasing age (Figure 4). Where phenocrysts are present, plagioclase and pyroxene predominate. The rocks are generally unaltered, except for pervasive oxidation and development of clays in the cinder-rich pyroclastic units.

Surprisingly, the volcanic sequence is interrupted by only one, thin sedimentary unit and no rhyolite units even though moat rhyolite volcanism was contemporaneous. The absence of even fragmental moat rhyolite material is significant in view of the proximity of the site to the Deer Mountain rhyolite dome. This dome and the other late west moat porphyritic rhyolites likely postdate the shallowest cored moat basalt flow.

The water table is at the base of the moat basalt section. The section is therefore cold and isothermal (Figure 5) due to downward percolation of rainwater.

**Gravels.** The thick sequence of gravels underlying the moat basalt sequence record a time of relative quiet in the west moat. Units within the sequence range from clast-poor sand layers to coarse conglomerates with clasts to 0.15 m. The typical material, however, consists of 10- to 15-mm clasts in a sand matrix and is unconsolidated. Clast lithologies are basement (both granitic and metamorphic), precaldern volcanic rocks (basaltic to dacitic), and both microcrystalline- and obsidian-textured early rhyolite. Proportions of each component vary widely and unsystematically through the sequence. Except for the early rhyolite component, the lithologies resemble those present on the San Joaquin Ridge, which forms the western topographic rim of the caldera. The deposits are likely those of an ancestral Deadman Creek that drained San Joaquin Ridge and picked up early rhyolite debris at lower eleva-

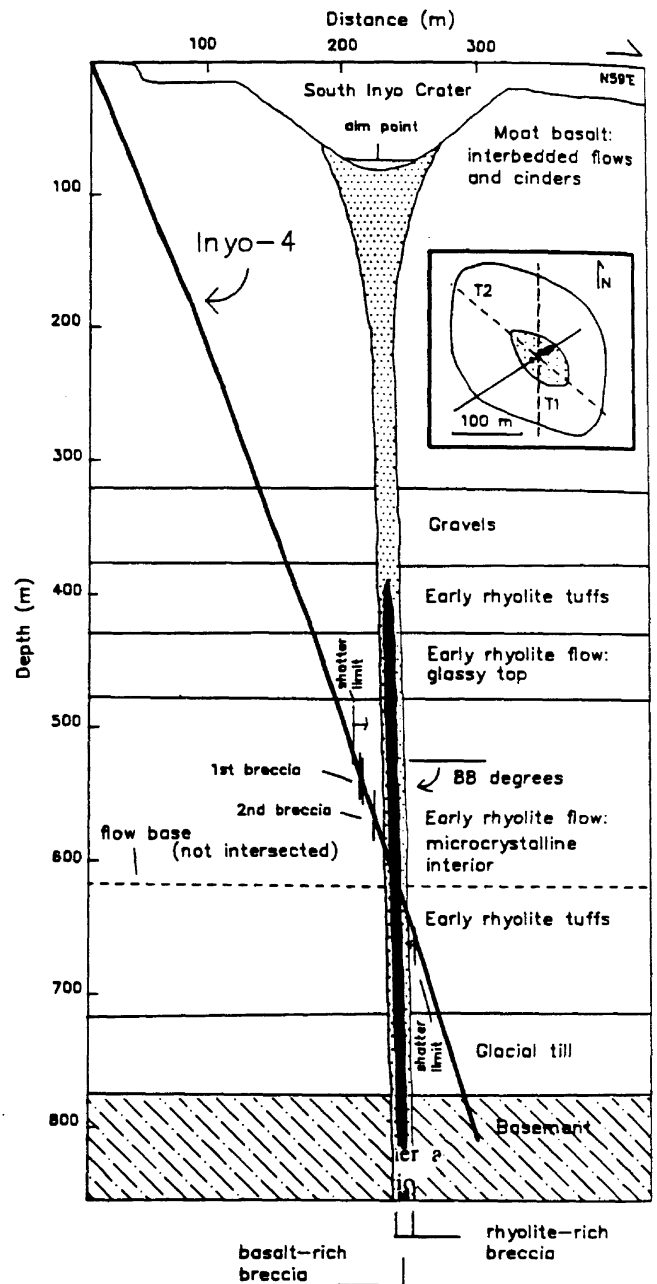


Fig. 2. Path of Inyo-4 in cross section with generalized stratigraphy and interpreted breccia structure. Inset shows the path of the hole (solid straight line) in plan view under the outline of the crater rim and crater lake. T1 and T2 are the main and subsidiary structural trends, respectively, as discussed in the text. Heavy bars on the path of the hole in the inset show where the breccia zones were intersected.

tions. Prominent obsidian and basement pebbles in the ejecta from the phreatic crater atop Deer Mountain probably came from this layer, as did basement pebbles in the South Inyo Crater ejecta.

**Early rhyolite.** The early rhyolite sequence encountered by Inyo-4 consists of five recognizable tuff units and a single massive flow. Tuff units range in thickness from 4 to 44 m, and results constrain the thickness of the flow to between 163 and 214 m. The units range from aphyric to finely and sparsely porphyritic. None are phenocryst-rich, and none are quartz-

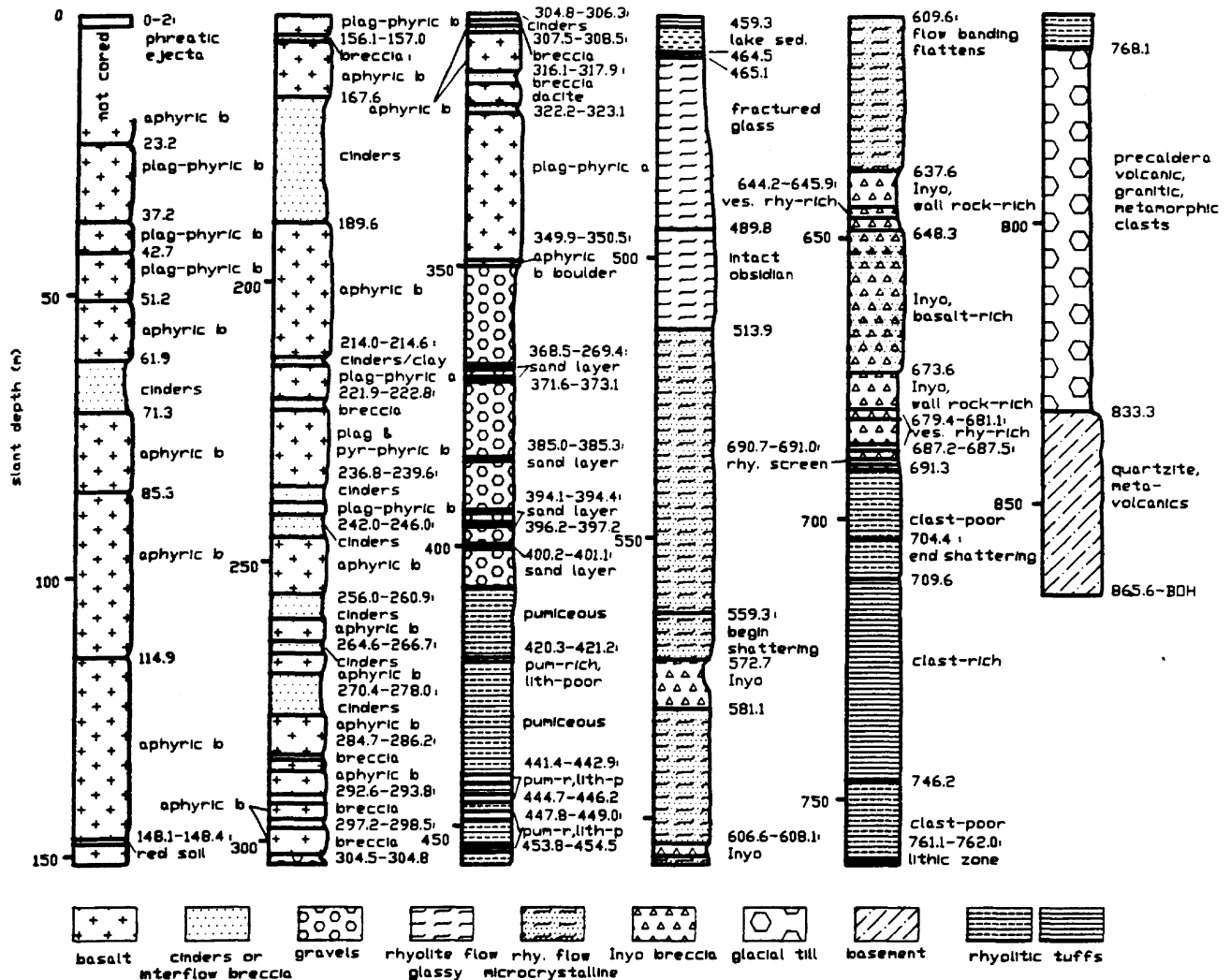


Fig. 3. Stratigraphy encountered by Inyo-4. Slant depths shown are reference values. For true slant depth from ground surface subtract 1.5 m for 0-175.2 m or 4.6 m for 175.2-865.6 m.

bearing. The tuffs are thoroughly altered to clays except for occasional intact obsidian or microcrystalline rhyolite clasts. There is abundant evidence of deposition and/or reworking in water provided by well-bedded sandy layers and rounded pumices. One 5-m-thick interval of varved lake sediments interrupts the sequence. The tuff units differ in pumice content and lithic content, but all are nonwelded.

The early rhyolite flow contains a few percent of 0.5- to 1-mm phenocrysts of plagioclase and subordinate pyroxene, biotite, and hornblende. Its vitrophyric portion texturally resembles Inyo lavas and tephros so closely that we initially interpreted this unit as the Inyo dike. The uppermost portion consists of yellow hydrated glass fractured on a millimeter scale. Faint flow banding at 20° to the core axis, consistent with a vertical orientation, is discernable. Two meters into the flow, nodules of residual fresh obsidian first occur and increase downward in abundance until, midway through the 46-m-thick glass zone, the flow is entirely intact obsidian. The downward transition from obsidian to microcrystalline rhyolite is abrupt, occurring over several centimeters. Flow banding is much more prominent in the microcrystalline rhyolite.

Gray and white layers are interbanded on a scale of millimeters. Although in places contorted, the flow banding generally maintains an acute angle to the core axis until 137 m into the flow, where the angle opens to 60°-70°, consistent with a near-horizontal orientation. Sulfides are abundant near the top of the microcrystalline zone and in areas of intense fracturing. Areas of chlorite deposition and of silica coatings on fractures are also present.

**Glacial till.** A 63-m-thick clastic unit, probably a glacial till, lies directly below the early rhyolite sequence. The unit contains clasts of precaldern volcanic rocks, granitic rocks, and metamorphic rocks in an unconsolidated clay matrix. Clast size ranges upward to 2 m. Clasts are angular to sub-round and some have striated surfaces.

**Basement.** The hole terminated in basement rocks that appear to represent a portion of the Mount Morrison [Rinehart and Ross, 1964] or Ritter Range [Huber and Rinehart, 1965] roof pendants. The core is approximately 60% massive brecciated quartzite cut by 40% chloritized porphyritic andesitic hypabyssal intrusives. Sulfides, carbonates, and epidote are abundant in fractures.

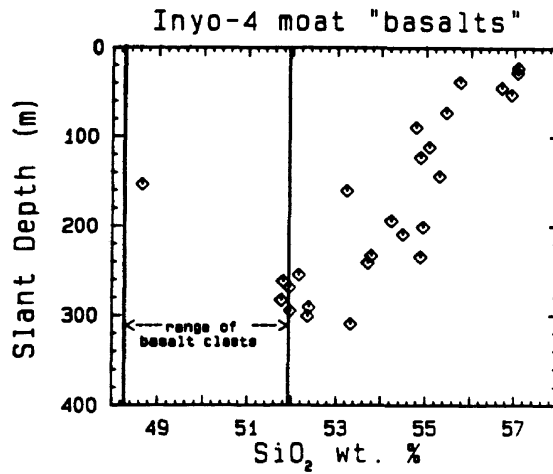


Fig. 4. Slant depth versus silica content for lavas of the moat basalt sequence. The lavas have become more evolved with time.

#### DISCUSSION OF STRATIGRAPHY

These results are surprising because they show shallow basement and absence of both the precaldera volcanic sequence and the Bishop Tuff at a locality 3–4 km within the topographic margin of the caldera. Moreover, they differ sub-

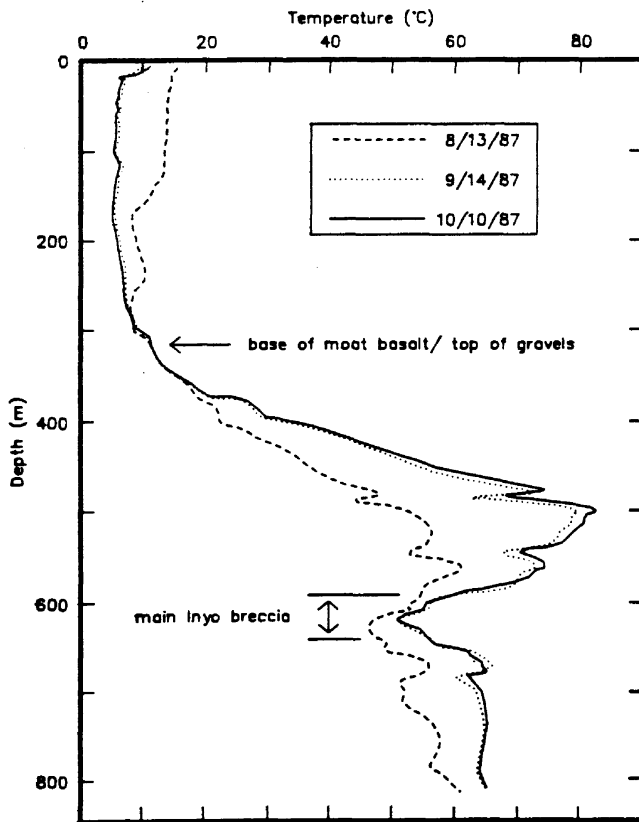


Fig. 5. Temperature logs for Inyo-4 run 1 day, 1 month, and 2 months after completion of the hole. A change from constant to steeply increasing temperature with depth occurs at the water table, which is at the base of the moat basalt section. A temperature minimum is located within the main breccia zone. Data obtained by R. Jacobson, Sandia National Laboratories.

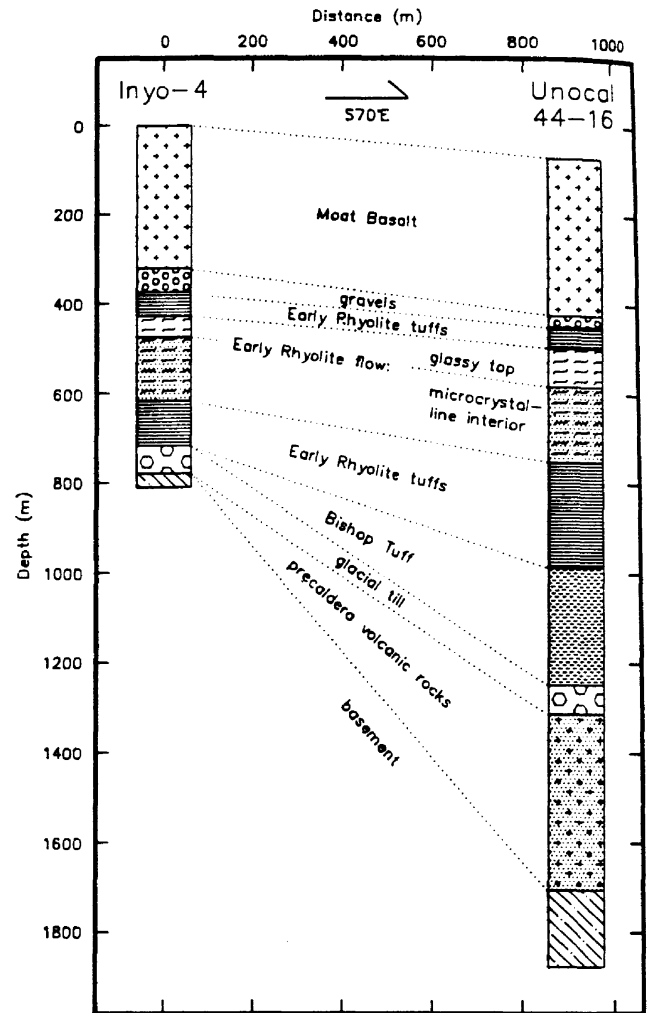


Fig. 6. Comparison of stratigraphic results of Unocal 44-16 [Suemnick, 1987] and Inyo-4. Zero depth is set at the ground surface at the Inyo-4 drill site. Note the large differences in the lower portion of the section but close similarity in the upper portion.

stantially from the results of Unocal Corporation's well IDFU 44-16 located only 900 m to the southeast (Figure 6) [Suemnick, 1987]. The two sections are very similar for the first 600 m. Both holes encountered a thick (321 m in Inyo-4 versus 378 m in 44-16) section of moat basalt and a layer of San Joaquin Ridge-derived gravels beneath the basalts reflecting a substantial hiatus in volcanic activity. Both holes also apparently encountered the same 200-m-thick rhyolite flow with its partially hydrated glassy top and distinctive, strongly flow-banded microcrystalline interior. Because the difference in elevation of contacts between these units resembles the difference in surface elevation, it appears that this region has not been greatly deformed since before eruption of the early rhyolite flow and that the gentle recent upwarp of the Inyo trend postdates the moat basalt eruptions.

Below the early rhyolite flow, the volcanic sequence in Inyo-4 is much thinner. The early rhyolite tuffs below the flow total less than half the thickness in Inyo-4 that is present in 44-16. The Bishop Tuff and precaldera volcanic lavas, which total about 700 m in 44-16, are absent in Inyo-4. However, a glacial till, presumed to be the Sherwin Till because of its

position immediately below the Bishop Tuff in 44-16 [Suemnicht, 1987], is present in both holes. Basement, in both cases metamorphic rocks such as occur in the Sierran roof pendants, is 900 m shallower in Inyo-4. These observations require that a major fault lies between the two wells. The fault has a down-to-the-east displacement of about 1 km, most of which occurred before eruption of the early rhyolite sequence was complete. The fault apparently forms a major part of the western structural boundary of the caldera 3-4 km east of its topographic expression. It is likely a southern extension of the Hartley Springs fault, as that fault trends into this area from the northwest margin of the caldera. This general configuration was proposed by L. Varga and G. A. Suemnicht (written communication, 1986), although Inyo-4 has more closely constrained the position of the bounding fault. Repeated activity on the fault until early postcaldera time would have maintained a scarp that led to ponding of volcanic units to the east and their absence by erosion or nondeposition to the west near its crest. The same situation exists farther north on the Hartley Springs fault outside the caldera where about 300 m of precaldra lavas and tens of meters of Bishop Tuff overlie the basement east of the scarp, but basement is exposed near and west of its crest. However, to account for the low elevation of the top of the Bishop Tuff in 44-16 and its absence in Inyo-4, it seems necessary to postulate foundering of the west moat after the Bishop eruption, presumably immediately after during the final stages of caldera collapse [Suemnicht, 1987]. This foundering produced the present western topographic margin of the caldera. Low temperatures in Inyo-4 (Figure 5) relative to 44-16, approximately 70°C cooler at the bottom-hole depth of Inyo-4, indicate that the fault is also a barrier to westward circulation of caldera thermal waters or that thermal waters rise along the fault and flow eastward. In either case, it appears that Inyo-4 is on the outer edge of the caldera structurally and thermally. Much of the west moat may be a cold, shallow shelf. These results are at variance with geologic interpretations of seismic data [Hill et al., 1985], perhaps because low-velocity roof-pendant rocks were erroneously assigned to caldera fill. The results are, however, consistent with Carle's [this issue] recent interpretation of gravity data.

An alternative interpretation of Inyo-4 results is that the basement encountered by the hole is a landslide block that moved eastward from newly formed caldera walls and lies on top of the Bishop Tuff. Suitable source lithologies are presently exposed on the western caldera rim [Huber and Rinehart, 1965; R. A. Bailey, personal communication, 1988]. Such blocks are known to occur in Long Valley [Suemnicht, 1987] and other calderas [Lipman, 1984]. It was decided not to test this possibility by further drilling because drilling conditions were becoming increasingly difficult and no meaningful constraint could be placed on the additional depth needed to establish with certainty that the basement was not a landslide. It is important to note, however, that a thin landslide flake would not be expected to depress the temperatures in Inyo-4 relative to those in 44-16 and that no clasts of the missing Bishop Tuff and precaldra lavas have been recognized in the intrusive breccias described below.

Knowledge of the stratigraphy can be used to constrain the depth of derivation of the crater ejecta. Small fragments of strongly flow-banded microcrystalline rhyolite in the ejecta texturally and chemically match the crystalline interior of the early rhyolite flow, requiring that excavation of material ex-

tended to at least 500 m depth. The only plausible source of large granitic blocks in the ejecta is the glacial till at 700 m depth. The shallower gravels contain granitic clasts but not any nearly as large as some in the ejecta. Finally, abundant small clasts of metaquartzite probably came from the basement at depths of 800 m or more.

#### INYO BRECCIAS

Three breccia zones interrupt the stratigraphy described above. In horizontal projection (Figure 2) they occur from 12.0 m southwest to 25.1 m northeast of the center of South Inyo Crater. If interpreted as vertical structures, their intersected widths are, from southwest to northeast, 2.7, 0.4, and 16.6 m. The early rhyolite wall rock is intensely shattered beginning 4.3 m southwest of the first breccia zone and extending 4.0 m past the third. The breccias consist of 25-75% clasts set in a fine, light gray matrix. Four types of clasts are apparent.

**Basalt.** This is a dark gray, fine- to medium-grained, fresh-appearing basalt. It contains sparse 1- to 5-mm phenocrysts of plagioclase and iddingsitized olivine. It is extremely dense except in the first (southwest) breccia zone and a few clasts in the outer portion of the main (northeast) breccia zone. The texture is distinct from that of the moat basalt lavas in its coarser crystallinity and characteristically low porosity. Clasts are rounded, angular, or irregularly shaped and range in size from a few millimeters to one meter in intersected length (Figure 7). Chemically, the clasts are transitional between high-alumina and trachybasalt and show considerable variation in the trace elements Cr and Ni (Table 1).

**Flow-banded microcrystalline rhyolite.** These clasts are identical to the adjacent interior of the early rhyolite flow, which is the only microcrystalline rhyolite lava present in the stratigraphic section. The clasts exhibit the same phenocryst assemblage and prominent flow banding. They are angular in shape and range in size from a few millimeters to about 0.1 m (Figure 7).

**Basement.** Fragments of both metamorphic and granitic rocks are present in the breccias. They are angular to sub-round and range upward in size to about 0.1 m.

**Vesicular silicic clasts.** The presence of vesicular silicic glass (Figure 8) is distinctive and significant in that this texture does not occur outside the breccias in the volcanic section (pumices in the early rhyolite tuffs are altered to clay). Gradations within large clasts show that the glassy clasts are the unaltered subset of variably devitrified and variably argillized vesicular silicic clasts. This component makes up a significant proportion (probably  $\gg 10$  vol %, but an accurate proportion cannot be determined due to the very large size range of fragments and the difficulty in identifying the smallest fragments) of the breccia throughout the main zone and reaches proportions  $> 80$  vol % in the slant depth intervals 644.2-645.9, 679.4-681.1, and 687.2-687.5 m (Figure 3). Shape varies from rounded to highly irregular, or occasionally angular. Color varies from yellow to green to dark gray. Porosity varies from  $> 50\%$  to near 0%. Clasts range upward in size to 0.2 m. In general, larger clasts and denser clasts are less altered. Relative to glassy portions of large clasts, nonglassy zones exhibit lowered silica content, increased alumina content, and large changes in the K/Na ratio. These changes appear to reflect formation of sanidine by devitrification and of clay by hydrothermal alteration. Consequently, only data from glassy clasts or glassy areas of clasts can be considered to reflect



Fig. 7. Representative samples of the rhyolite-rich marginal zone of the main breccia unit (top; slant depth = 680.3 m) and basalt-rich central zone (bottom; slant depth = 664.2 m). Arrows on the sample from the marginal zone point to a basalt clast (left) and a vesicular silicic clast (right). Note that in the central zone sample, both irregular and angular basalt clasts (dark clasts) occur. In both samples, the white to gray, banded, medium-size clasts are early rhyolite wall rock. The marginal zone sample is from a continuous unit of similar characteristics, but the central zone sample probably represents a fracture filling between much larger blocks (to 1 m) of basalt. The scale is in centimeters.

magmatic composition. That composition is high-silica rhyolite (Table 1). All of the glass is hydrated, as indicated by low analytical totals (both by electron microprobe and XRF), so chemical changes due to hydration cannot be eliminated from the data set. The clasts are sparsely porphyritic, with phenocrysts of  $An_{30}$  plagioclase up to 3 mm in length.

The clasts are set in a matrix of 0.01- to 0.1-mm particles that are coated with clay (Figure 9). The particles consist of microcrystalline rhyolite and vesicular silicic microclasts, with subordinate basalt blebs and basement-derived crystal grains. The particles are loosely to firmly cemented together, always leaving substantial void space between grains.

The main breccia unit exhibits a symmetrical zonation (Figure 10). The margin zones are matrix-rich (~75%), clasts of flow-banded microcrystalline rhyolite and vesicular rhyolite glass predominate, and basalt clasts are very much subordinate (Figure 7). Clasts are typically  $\leq 0.1$  m. The central zone is matrix-poor (~25%) and rich in very large (to 1 m) basalt clasts (Figure 7).

#### INYO EJECTA

Two samples of the ejecta deposit from South Inyo Crater were collected for comparison with the Inyo breccias. The

samples came from the northeast crater wall where the deposit is thickest, about 20 m, and consists of alternating layers, 2-3 m in thickness, of explosion breccia, fallout, and base-surge tephra. They were taken from a surge dune near the base of the deposit and from a massive tephra layer near the top. Both samples may be classified as lithic tuff.

The samples contain nearly 50 vol % matrix ash less than about 50  $\mu$ m in diameter, 25-30 vol % lithic clasts ranging in size from <1 mm to block-size fragments, 15-20 vol % glass shards from 0.1 to 0.5 mm in diameter, and 6-7 vol % crystal grains (Table 2). By far, basalt lava and subordinate basalt scoria dominate the lithic clast population. The basalt lava is pilotaxitic, plagioclase being the dominant phenocryst with minor olivine and pyroxene. The basalt scoria is hyalocrystalline. Rhyolite is present as devitrified and hydrothermally altered clasts, as rounded obsidian clasts, and as newly discovered blocky and equant shards containing spherical vesicles (Figure 8).

#### DISCUSSION OF INYO BRECCIAS AND EJECTA

A number of breccia or breccialike units exist or may exist beneath the Inyo Craters area that bear no relationship to the craters. These include lithic tuffs, fault gouge, fault talus, gla-

TABLE 1. Chemical Compositions of Samples From South Inyo Crater and the Inyo Domes

	South Inyo Crater*								Inyo Domes†											
	mb(26) Whole Rock		bc(12) Whole Rock		er(6) Whole Rock		vsc(6) Whole Rock		vsc(20) Microprobe		ejecta(9) Microprobe		fp-1(36) Whole Rock		fp-2(41) Whole Rock		cp(9) Whole Rock		fp-1(1) Microprobe	
	Mean	S.D.	Mean	S.D.	Mean	S.D.	Mean	S.D.	Mean	S.D.	Mean	S.D.	Mean	S.D.	Mean	S.D.	Mean	S.D.	Mean	S.D.
<i>Percent Anhydrous</i>																				
SiO <sub>2</sub>	55.02	1.95	50.83	0.31	75.36	0.36	74.80	0.68	76.18	0.66	76.18	0.03	73.70	0.22	71.48	0.90	71.72	0.36	73.73	
TiO <sub>2</sub>	1.61	0.14	1.79	0.12	0.21	0.01	0.22	0.01	0.15	0.03	0.11	0.05	0.14	0.009	0.27	0.07	0.35	0.01	0.17	
Al <sub>2</sub> O <sub>3</sub>	17.89	0.59	17.90	0.83	13.89	0.12	14.08	0.74	13.76	0.23	13.59	0.52	14.15	0.12	14.96	0.32	14.64	0.18	14.71	
FeO(t)	7.51	0.38	8.87	0.49	0.92	0.22	1.49	0.21	1.01	0.18	1.06	0.14	1.47	0.12	2.03	0.30	2.08	0.10	1.27	
MnO	0.12	0.06	0.19	0.04	0.02	0.01	0.06	0.01	...	...	...	...	0.06	0.002	0.06	0.009	0.05	0.005	...	
MgO	4.10	0.90	6.34	1.16	0.18	0.12	0.19	0.16	0.08	0.04	0.08	0.05	0.02	0.02	0.23	0.12	0.56	0.03	0.06	
CaO	7.14	0.92	8.73	0.47	0.84	0.14	1.40	0.08	0.67	0.09	0.61	0.09	0.82	0.03	1.26	0.29	1.63	0.10	0.63	
Na <sub>2</sub> O	4.20	0.24	3.50	0.26	3.05	0.35	2.85	0.30	3.11	0.36	2.93	1.05	4.32	0.07	4.55	0.14	4.32	0.08	4.00	
K <sub>2</sub> O	1.94	0.33	1.35	0.19	5.51	0.26	4.88	0.68	5.04	0.75	5.44	0.59	5.29	0.07	5.09	0.18	4.54	0.13	5.48	
P <sub>2</sub> O <sub>5</sub>	0.46	0.03	0.49	0.02	0.03	0.005	0.03	0.007	...	...	...	...	0.03	0.002	0.07	0.02	0.10	0.004	...	
Totals	98.17		97.38		95.68		96.22		93.66		92.89		98.94		98.86		98.67		99.03	
<i>Parts Per Million</i>																				
Cr	10	11	99	80	...	...	...	...	...	...	...	...	...	...	...	...	...	...	...	...
Ni	19	27	105	78	...	...	...	...	...	...	...	...	...	...	...	...	...	...	...	...
Cu	27	12	32	15	...	...	...	...	...	...	...	...	...	...	...	...	...	...	...	...
Zn	89	4	101	22	20	7	58	12	...	...	...	...	...	...	...	...	...	...	...	...
Rb	28	10	24	7	147	12	205	63	...	...	...	...	158	6	138	7	116	4	...	...
Sr	923	98	906	112	128	12	236	28	...	...	...	...	40	7	134	46	251	23	...	...
Y	25	2	25	2	14	2	15	2	...	...	...	...	24	2	25	2	17	1	...	...
Zr	193	8	187	6	183	4	191	7	...	...	...	...	220	6	279	26	222	18	...	...
Nb	9	1	11	2	16	3	15	1	...	...	...	...	19	3	18	3	20	1	...	...
Ba	980	160	830	170	1209	84	1360	140	...	...	...	...	350	46	790	160	820	80	...	...

Numbers in parentheses are number of samples. Major elements reported anhydrous because of variable hydration: totals given for comparison. S.D., standard deviation.

\*Moat basalt (mb), basalt clasts (bc), early rhyolite (er), and vesicular silicic clasts (vsc) samples are from drilling; ejecta samples are surface samples.

†The fp-1, and fp-2 are finely porphyritic low-Ba and high-Ba samples from drilling at Obsidian dome [Vogel *et al.*, 1987]; coarsely porphyritic samples are surface samples at Deadman and Glass Creek domes.

cial till, and the vent breccias of much older, buried vents. Therefore it is necessary to consider carefully the relationships of the intersected breccias to each other, to the stratigraphy, and to the overlying crater before attempting to interpret the character of magmatic behavior that they represent.

**Correlation of the breccias.** All three breccia zones appear to consist of the same components. If an exception exists, it is the first breccia zone which contains a higher proportion of vesicular, rather than dense, basalt clasts and a significant amount of silicic glass particles in the matrix. Because of their similarity, it is appropriate to consider the origin of the three breccias together rather than singly.

**Intrusive or extrusive character of the breccias.** It is not possible to determine from a single core hole what the orientation of intersected features is without reference to the characteristics and stratigraphic sequence of the features. The cross section of a core is too small a sample of a contact to suggest whether the overall contact might be horizontal, vertical, or oblique. Among common igneous materials, the sampled breccias most closely resemble lithic ash flow tuffs. Figure 11 displays schematically the two most likely cases: that the breccias are intrusive vent breccias or extrusive lithic tuffs. Given that the breccias were formed in the same event, as proposed above, they must be intrusive. Horizontal extrusive layers separated by other units could not be contemporaneous. Nevertheless, we can lay aside the previous conclusion and consider the relationship of the breccias to the adjacent stratigraphic units. The first two breccias are in contact with the same unit,

the early rhyolite flow, at both their uphole and downhole margins. Therefore they must be intrusive into this unit. The third and largest breccia zone is in contact with the early rhyolite flow at its uphole margin and with an early rhyolite tuff at its downhole margin. However, it contains clasts of the early rhyolite flow throughout, extending to its downhole contact with the tuff. This could only be the case if the breccia is intrusive. If the breccia were erupted on top of the tuff, it could not contain fragments of the early rhyolite flow which would not yet have been in existence.

**Relationship of the breccias to the crater.** Because there are numerous vents in the area that are related to moat basalt and early rhyolite eruptions, it is possible that the breccias could be related to vents much older than 600 years. However, the ejecta from the crater contains the same components as the breccias (Table 2), including, as will be discussed, the high-silica vesicular glass clasts which are absent from the wall rock stratigraphy (Figure 8). It is also important to note that the intersected breccias are closely centered under the crater (Figure 2), making it highly probable that they represent the feeder for the crater.

**Evidence for the juvenile magmatic component.** The excavation of a large volcanic crater almost certainly requires a close spatial relationship to magmatic heat. Accordingly, core samples of rhyolite petrographically resembling Inyo lavas and tephra were quickly analyzed as drilling proceeded. No materials chemically matching known Inyo eruptives (Table 1) [Vogel *et al.*, 1987; Sampson and Cameron, 1987] were found.

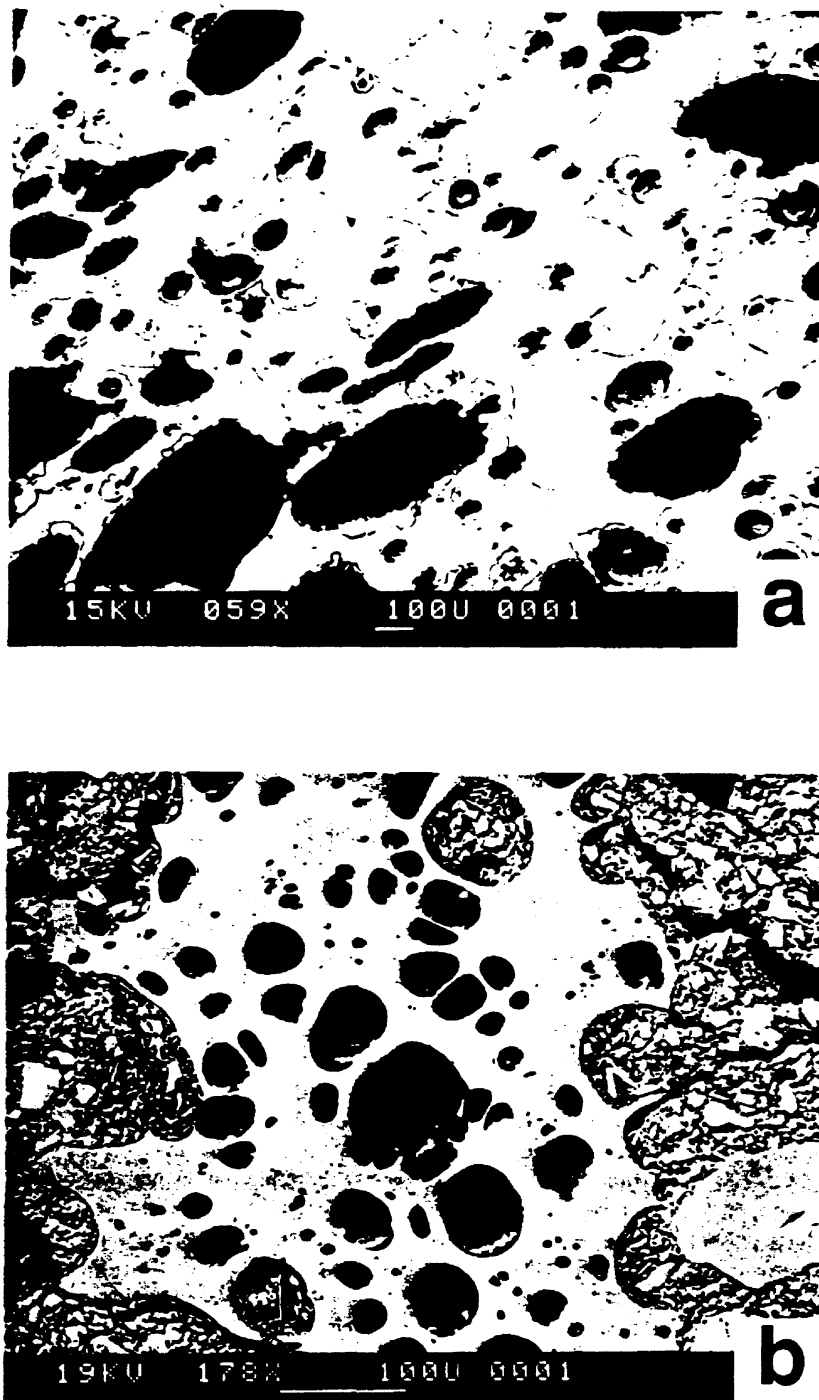


Fig. 8. Scanning electron microscope photomicrographs of (a) fresh-appearing glassy vesicular silicic clasts from the main breccia zone (slant depth = 643.0 m) and (b) the crater ejecta. Both samples are hydrated but otherwise unaltered, except for ragged selvages visible on the walls of vesicles in the breccia clast. The selvages are areas of incipient devitrification.

nor have any been found subsequently, indicating either that juvenile material is absent from the breccias or that the juvenile component is of a composition different from the magma that reached the surface in the northern part of the Inyo chain. The stratigraphic results indicate that the hole sampled the entire volcanic section. Therefore the juvenile component, if present as clasts, will be those volcanic clasts that do not match any of the intersected volcanic wall rocks. The two clast

types meeting this criterion are the vesicular silicic clasts and the dense basalt.

If the basalt clasts had dropped >300 m downward from the moat basalt section, the only possible source of basalt in the wall rock, a large range of vesicle contents and crystallization textures would be expected. Instead, the generally low vesicularity and medium-grained crystallinity of the clasts suggest an intrusive environment of emplacement. The basalt

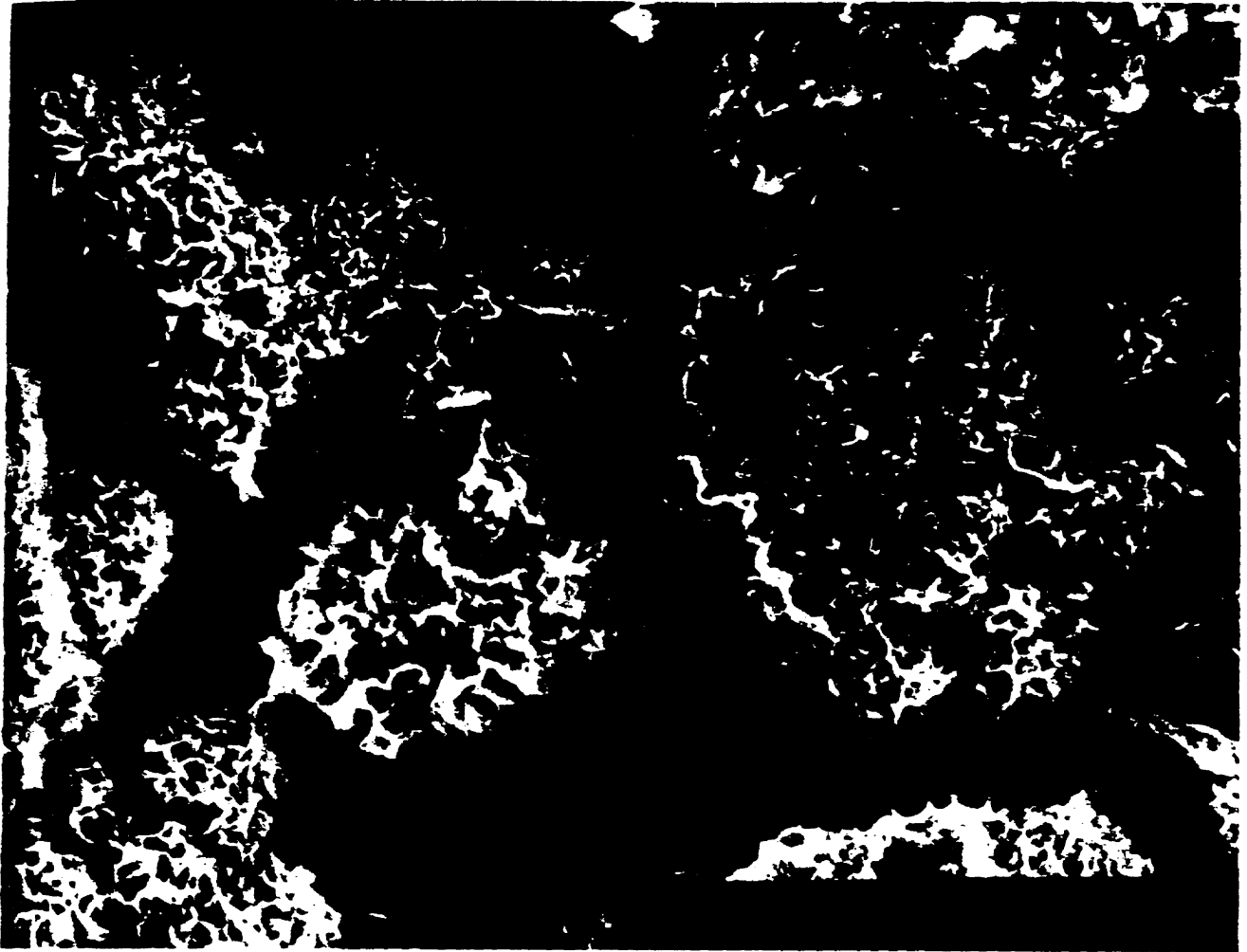


Fig. 9. Smectite overgrowths on 10- to 30- $\mu\text{m}$  particles comprising the matrix of the breccia (slant depth = 643.5 m). The overgrowths and substantial void space between grains are general characteristics of the breccia. Scale bar is 10  $\mu\text{m}$ . Scanning electron microscope photomicrograph by J. L. Krumhansl, Sandia National Laboratories.

could represent a 600-year-old magma that intruded and fragmented in the wet caldera fill, thereby causing the phreatic eruptions [Eichelberger *et al.*, 1987]. Such an interpretation was suggested by the central position of the basalt within the main breccia zone (Figure 10), crenulate or fluidal appearing borders on some basalt clasts (Figure 7), and rinds on some clasts that could represent chilling. We subsequently obtained K/Ar ages of  $380 \pm 100$  kyr and  $260 \pm 400$  kyr on material from a large, centrally located, fresh-appearing clast. Although the large sigma values in these determinations require caution, the nonzero ages indicated the need to reevaluate the basalt hypothesis. If blobs of molten basalt were present in a rapidly rising slurry 600 m beneath a vent, then some of this material would be expected to appear as quenched glass pyroclasts in the ejecta. Careful inspection of the ejecta has yielded no more than a single candidate grain, which might well have been derived from one of the eight basaltic pyroclastic units within the moat basalt sequence. Rinds on the basalt breccia clasts do not contain glass and may have developed by alteration rather than chilling. Planar breaks in the basalt with injections of breccia matrix are more common than fluidal clasts. The former suggests fragmenting of cold rock, while the latter may

result from oblique sections through irregular surfaces. In composition, the clasts lie at the primitive end of the moat basalt trend (Figure 12). Considering the chemical variation with time (Figure 4), we interpret the basalt clasts as representing an early feeder for the moat basalt sequence, which was shattered by a later event. The total of the intersected intervals of basalt in the main breccia zone would comprise a dike 3.6 m in horizontal width along the azimuth of the hole. If the dike is aligned north-south, like the present Inyo chain, its true thickness would be 2.8 m. This thickness is a lower limit, as it neglects the smaller fragments lost during coring of the breccia.

From the standpoint of texture, the pumicelike vesicular silicic clasts represent the most likely candidate for juvenile material. Because the only glass in the wall rock section is the glassy carapace (and probably base) of the early rhyolite flow, the only possible nonjuvenile origin for glassy vesicular clasts in the breccia is that it is flow glass heated above its softening point and thereby vesiculated. Significant chemical differences between vesicular silicic clasts and flow glass, including a factor of 2 difference in Sr concentrations (Table 1 and Figure 13), makes this origin seem unlikely. The vesicular silicic clasts

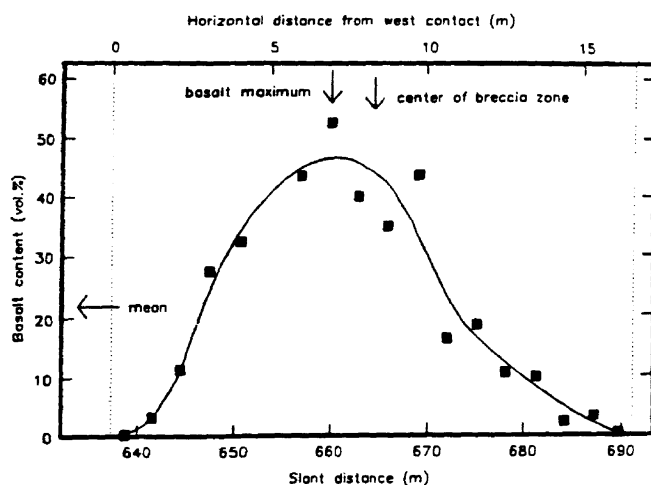


Fig. 10. Basalt content as a function of position across main breccia zone. Basalt content was determined over 10-foot (3-m) intervals of drilled distance by summing lengths of basalt clasts measured along the core axis and dividing by 10 feet. This approach was used because core recovery was quite low through the basalt-rich zone and drilling characteristics indicated that the material lost was breccia matrix.

are, however, clearly distinct from previously recognized Inyo eruptives as well (Figure 13).

For the crater ejecta the possible nonjuvenile ("juvenile" in the strictest sense of new magma from the same vent as the deposit) sources of vesicular silicic clasts are reheating of early rhyolite obsidian, for which we find no evidence, or reworking of the immediately underlying ~1 m of Inyo air fall tephra. The tephra came from the Deadman Dome and Glass Creek vents [Miller, 1985] and both the finely porphyritic and coarsely porphyritic magma types [Bailey et al., 1976; Sampson, 1987; Sampson and Cameron, 1987] are represented. The clasts in the crater ejecta cannot be the coarsely porphyritic Inyo phase because they are not porphyritic. The electron microprobe analyses in Table 1 show them to be distinct from the crystal-poor finely porphyritic phase as well (the comparison is made with the highest-silica finely porphyritic material). They do, however, match the vesicular silicic clasts from the breccia. We therefore infer that the vesicular silicic clasts in the breccia and ejecta represent the magma that caused the development of the Inyo Craters and that this magma is distinct from the magmas that contemporaneously vented in the northern part of the chain.

Three caveats should be stated pertaining to this interpretation. First, we have not yet found  $An_{30}$  phenocrysts, such as

TABLE 2. Modes for Ejecta Samples

Constituent	Lower	Upper
Matrix	51.7	45.9
Rhyolite glass	15.2	17.3
Rhyolite-crystalline	11.6	3.0
Basalt	14.1	25.1
Metaquartzite	1.1	1.9
Quartz	3.0	1.7
Alkali feldspar	0.8	1.4
Plagioclase	1.9	2.5
Hornblende	0.2	0.6
Biotite	0.2	0.2
Olivine	...	0.2
Pyroxene	0.2	0.2

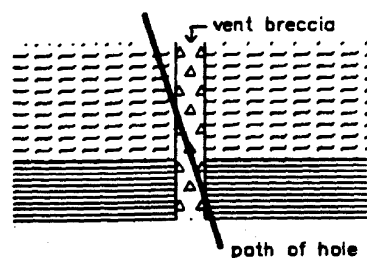
In volume percent.

occur sparsely in the vesicular silicic clasts in the breccia, in the ejecta. The abundance of wall rock-derived crystal grains and the small size scale of fragmentation of juvenile material relative to the spacing of phenocrysts means that juvenile clasts containing both phenocrysts and glass will be hard to find, but they should be present. Second, the vesicular and nonvesicular glass in the crater ejecta cannot be distinguished from early rhyolite or from each other on the basis of electron microprobe analyses, but a whole rock trace element comparison is not possible because of the small size of the pyroclasts. Probably some of the nonvesicular glass is early rhyolite, so the juvenile component of the ejecta is less than the 15–17 vol % glass reported in Table 2 but not less than the proportion of vesicular glass (~1 vol %), which can be judged to be juvenile on the basis of texture. Third, composition of the glass in the breccia and ejecta has been affected by hydration (as the variance in  $Na_2O$  in the ejecta glass indicates), and the effect is not accurately known. It is unlikely, however, that this effect has made the breccia and crater glasses similar and these two sets dissimilar from the northern Inyo glasses.

#### CONCLUSIONS

We conclude that the Inyo Craters eruption was caused by the rise of high-silica rhyolite magma along the path of an older feeder for the moat basalt sequence. Although this magma is chemically distinct from the magmas that vented contemporaneously to the north, it remains possible that the dike structure under the chain is continuous and was fed from multiple magma reservoirs. Vesiculation and fragmentation of the magma began at a depth greater than 600 m, where the crater feeder was intersected by drilling. Vesiculation at this

#### Intrusive case:



#### Extrusive case:

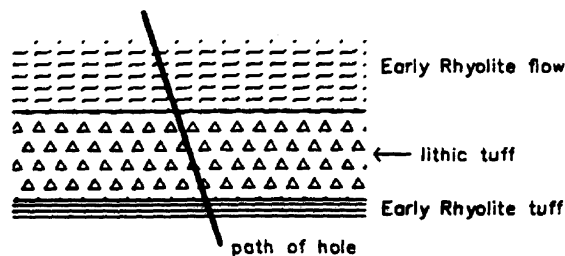


Fig. 11. Schematic illustration of the two cases for interpretation of the main breccia unit permitted by the sequence in which units were encountered.

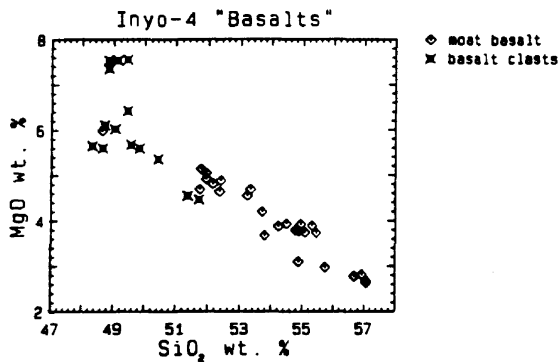


Fig. 12. Comparison of the compositions of moat basalt lavas and basalt clasts from the breccias, in terms of MgO versus SiO<sub>2</sub>. The clasts fall at the primitive end of the moat basalt trend.

depth implies substantial water content of the magma. For example, the 33 vol % bubble content of the clast shown in Figure 9a (based on 1000 points counted) implies a total water content (in melt + vapor) at the time of quenching of 2.2 wt % (assumes equilibrium between vapor pressure and lithostatic load, overburden density of 2.5 g/cm<sup>3</sup> [Sparks, 1978]). This is clearly ample to drive a high-velocity Plinian eruption [Wilson, 1980]. However, the modest vesicularity of many of the juvenile clasts and large proportion of lithic material in both the conduit and ejecta suggest that heating and vaporization of groundwater, with corresponding chilling of the magma, played an important role in the eruption. Because the ejecta appears to contain juvenile material but the activity has a strong phreatic character, the eruption can be termed phreatomagmatic.

The drilling results show that the Inyo feeder is fragmental beneath South Inyo Crater at a depth at which it is an intact intrusive outside the caldera. A comparison of intact intrusives inside and outside the caldera is therefore not possible. The Inyo breccias may be more analogous to lithic-rich, juvenile-clast-poor fracture fillings in basement near the dike outside the caldera [Heiken et al., 1988]. Furthermore, because the magma responsible for Inyo Craters is different from those vented to the north, we do not have the controlled experiment on the effect of geologic environment upon magmatic behavior for which we had hoped. The Inyo Craters high-silica rhyolite magma may have had a higher water content than the other rhyolite to rhyodacite Inyo magmas, causing it to frag-

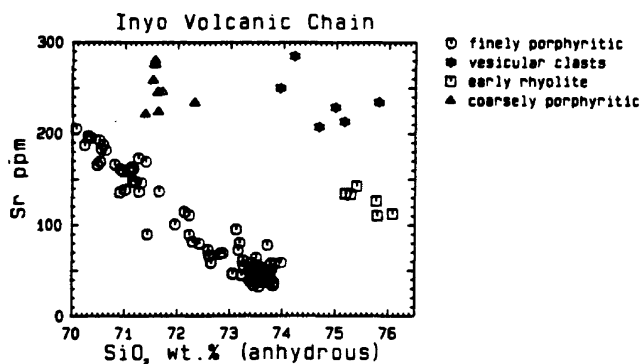


Fig. 13. Comparison of the compositions of glassy vesicular silicic clasts from the breccia with compositions of glassy early rhyolite and Inyo intrusive and eruptive units. The samples sets are the same as those described for Table 1.

ment at greater depth. Certainly, there is no support for the idea that the intruding magma degassed more rapidly within the caldera in view of the deeper level of fragmentation there, although fragmentation within the caldera could have been aided by external water. Nevertheless, the difference between the intracaldera and extracaldera environments remains an attractive hypothesis for explaining the difference in magmatic behavior. Intersection of wet caldera fill by rising magma beneath South Inyo Crater can account for the strongly phreatic character of its activity. Continued influx of groundwater then quenched the system at an early stage of evolution, preventing it from progressing to Plinian and then effusive activity.

The pervasive hydrothermal alteration of the breccia probably occurred during its cooling, immediately following emplacement. Temperature logs show that cooling is complete (Figure 5). Indeed, the presence of a temperature minimum within the main breccia zone indicates that the crater's conduit may serve as a pathway for cold water invasion. The absence of a persistent positive thermal anomaly and presence of only a small intrusive structure lend no support to the view that the Inyo event rejuvenated the Long Valley Caldera hydrothermal system [Blackwell, 1985].

The difference between the intrusion width postulated from surface extension [Mastin and Pollard, this issue] and the intrusive structure encountered by drilling poses a problem. The total intersected width of Inyo breccias is 19.7 m. If the breccia is dikelike, dips 88° east (Figure 2), and strikes along the Inyo trend, its true width is 15.1 m. However, much of this width is locally derived wall rock, which does not contribute to extension. Taking the juvenile component of the breccia as 10–50 vol % (the upper limit assumes that all of the matrix of the rhyolite-rich margin of the main breccia and half the matrix of the basalt-rich center of the main breccia are juvenile), the intact intrusive equivalent of the breccias is 2–8 m. This is no larger than the portion of the Inyo dike intersected by Inyo-3, which produced no noticeable surface deformation (some deformation may be concealed by the much greater thickness of Inyo tephra at the Inyo-3 site), and much smaller than the postulated few tens of meters. There are a number of possible ways out of this dilemma. The hole may have intersected an anomalously thin portion of the intrusion, although results at Obsidian Dome would suggest that the structure should be anomalously thick, not anomalously thin, under a vent. The intrusion could be much thicker at greater depth, below the level of fragmentation. If that is the case, then the breccias represent pyroclastic leaks up fractures above the main intrusion. It is also possible that the surface deformation at Inyo Craters is not solely the result of magmatic intrusion. Accompanying motion of the large fault just east of the site, together with differential compaction of caldera fill due to the nearly 1-km difference in depth to basement across the structure, could have contributed to the large local surface extension.

**Acknowledgments.** Drilling of Inyo-4 was funded by the U.S. Department of Energy, Office of Basic Energy Sciences (DOE/OBES), as part of the Continental Scientific Drilling Program. Support for research related to the drilling was provided by DOE/OBES (to J. C. E., T. A. V., L. W. Y., G. H. H., and K. H. W.) and by the U.S. Geological Survey (to C. D. M.). R. Jacobson of DOE's Geoscience Research Drilling Office at Sandia National Laboratories ably directed logistics and drilling, which was skillfully conducted in the highly fragmental formations by L. Pisto and his crew from Tonto Drilling Company. The operation would not have been possible without the following additional scientists who contributed their time and expertise as well sitters: C. Carrigan (Sandia), D. Emerson (Livermore), J. Krumhansl

(Sandia), L. Mastin (Stanford), V. McConnell (Sandia), J. Mills (Michigan State U.), M. Naney (Oak Ridge), R. Ryerson (Livermore), W. Sawka (Livermore), and H. Stockman (Sandia). V. McConnell also assisted with preparation of the figures. K/Ar age determinations were conducted by Allen Deino at the Berkeley Geochronology Center.

## REFERENCES

- Bailey, R. A., Chemical evolution and current state of the Long Valley magma chamber, Proceedings of workshop XIX: Active tectonic and magmatic processes beneath Long Valley Caldera, eastern California, edited by D. P. Hill, R. A. Bailey, and A. S. Ryall, *U.S. Geol. Surv. Open File Rep.*, 84-939, 24-40, 1984.
- Bailey, R. A., G. B. Dalrymple, and M. A. Lanphere, Volcanism, structure, and geochronology of Long Valley Caldera, Mono County, California, *J. Geophys. Res.*, 81, 725-744, 1976.
- Blackwell, D. D., A transient model of the geothermal system of Long Valley Caldera, California, *J. Geophys. Res.*, 90, 11,229-11,241, 1985.
- Carle, S. F., Three dimensional gravity modeling of the geologic structure of Long Valley Caldera, *J. Geophys. Res.*, this issue.
- Eichelberger, J. C., P. C. Lysne, and L. W. Younker, Research drilling at Inyo Domes, Long Valley Caldera, California, *Eos Trans. AGU*, 65, 721, 723-725, 1984.
- Eichelberger, J. C., P. C. Lysne, C. D. Miller, and L. W. Younker, Research drilling at Inyo Domes, California: 1984 results, *Eos Trans. AGU*, 66, 186-187, 1985.
- Eichelberger, J. C., C. R. Carrigan, H. R. Westrich, and R. H. Price, Nonexplosive silicic volcanism, *Nature*, 323, 598-602, 1986.
- Eichelberger, J. C., L. W. Younker, T. A. Vogel, and C. D. Miller, Coring beneath Inyo Craters, Long Valley caldera, California (abstract), *Eos Trans. AGU*, 68, 1544, 1987.
- Fink, J. H., Geometry of silicic dikes beneath the Inyo Domes, California, *J. Geophys. Res.*, 90, 11,127-11,134, 1985.
- Fink, J. H., and D. D. Pollard, Ground cracks as indicators of geothermal potential (abstract) *Eos Trans. AGU*, 64, 898, 1983a.
- Fink, J. H., and D. D. Pollard, Structural evidence for dikes beneath silicic domes, Medicine Lake Highland volcano, California, *Geology*, 11, 458-461, 1983b.
- Heiken, G. H., K. H. Wohletz, and J. C. Eichelberger, Fracture fillings and intrusive pyroclasts, Inyo Domes, California, *J. Geophys. Res.*, 93, 4335-4350, 1988.
- Hill, D. P., E. Kissling, J. H. Luetgert, and U. Kradolfer, Constraints on the upper crustal structure of the Long Valley-Mono Craters volcanic complex, eastern California, from seismic refraction measurements, *J. Geophys. Res.*, 90, 11,135-11,150, 1985.
- Huber, N. K., and C. D. Rinehart, Geologic map of the Devils Postpile quadrangle, Sierra Nevada, California, *U.S. Geol. Surv. Geol. Quad. Map*, GQ-437, 1965.
- Lipman, P. W., The roots of ash flow calderas in western North America: Windows into the tops of granitic batholiths, *J. Geophys. Res.*, 89, 8801-8841, 1984.
- Mastin, L. G., and D. D. Pollard, Surface deformation and shallow dike intrusion processes at Inyo Craters, Long Valley, California, *J. Geophys. Res.*, this issue.
- Miller, C. D., Holocene eruptions at the Inyo volcanic chain, California—Implications for possible eruptions in the Long Valley caldera, *Geology*, 13, 14-17, 1985.
- Reches, Z., and J. Fink, The mechanism of intrusion of the Inyo Dike, Long Valley Caldera, California, *J. Geophys. Res.*, 93, 4321-4334, 1988.
- Rinehart, C. D., and D. C. Ross, Geology and mineral deposits of the Mount Morrison Quadrangle, Sierra Nevada, California, *U.S. Geol. Surv. Prof. Pap.*, 385, 106 pp., 1964.
- Sampson, D. E., Textural heterogeneties and vent area structures in the 600-year-old lavas of the Inyo volcanic chain, eastern California, The Emplacement of Silicic Domes and Lava Flows, edited by J. H. Fink, *Spec. Pap. Geol. Soc. Am.*, 212, 89-100, 1987.
- Sampson, D. E., and K. L. Cameron, The geochemistry of the Inyo volcanic chain: Multiple magma systems in the Long Valley region, eastern California, *J. Geophys. Res.*, 92, 10,403-10,421, 1987.
- Sparks, R. S. J., The dynamics of bubble formation and growth in magmas: A review and analysis, *J. Volcanol. Geotherm. Res.*, 3, 1-37, 1978.
- Suennicht, G., Results of deep drilling in the western moat of Long Valley, California, *Eos Trans. AGU*, 68, 785, 798, 1987.
- Vogel, T. A., L. W. Younker, and B. C. Schuraytz, Constraints on magma ascent, emplacement, and eruption: Geochemical and geological data from drill-core samples at Obsidian Dome, Inyo Chain, California, *Geology*, 15, 405-408, 1987.
- Westrich, H. R., H. W. Stockman, and J. C. Eichelberger, Degassing of rhyolitic magma during ascent and emplacement, *J. Geophys. Res.*, 93, 6503-6511, 1988.
- Wilson, L., Relationships between pressure, volatile content and ejecta velocity in three types of eruptions, *J. Volcanol. Geotherm. Res.*, 8, 297-313, 1980.
- Wood, S. H., Distribution, correlation, and radiocarbon dating of late Holocene tephra, Mono and Inyo Craters, eastern California, *Geol. Soc. Am. Bull.*, 88, 89-95, 1977.
- J. C. Eichelberger, Sandia National Laboratories, Albuquerque, NM 87185.
- G. H. Heiken and K. H. Wohletz, Los Alamos National Laboratory, Los Alamos, NM 87545.
- C. D. Miller, Cascades Volcano Observatory, U.S. Geological Survey, Vancouver, WA 98661.
- T. A. Vogel, Department of Geological Sciences, Michigan State University, East Lansing, MI 48824.
- L. W. Younker, Lawrence-Livermore National Laboratory, Livermore, CA 94550.

(Received January 22, 1988;  
revised May 4, 1988;  
accepted May 12, 1988.)